

SHEAR BEHAVIOR OF REINFORCED CONCRETE HAUNCHED BEAMS WITHOUT SHEAR REINFORCEMENT

Chenwei HOU^{*1}, Koji MATSUMOTO^{*2} and Junichiro NIWA^{*3}

ABSTRACT

This study aims to clarify the shear resistance mechanism of reinforced concrete haunched beams (RCHBs) without shear reinforcement. Three RCHBs with different positions of haunched portion and one RCHB with thicker concrete cover in the mid span were tested. The results demonstrated that the positions of bends in the tensile rebars highly influenced the crack propagations which caused the variation in the shear capacities due to different contributions of arch action in the beams. The thicker concrete cover affected the crack pattern but almost no effect on the shear capacity.

Keywords: RC haunched beam, shear capacity, crack pattern, inclined tensile bars, arch action

1. INTRODUCTION

Reinforced concrete haunched beams (RCHBs) are often used in simply supported and continuous bridges, structural portal frames, mid-rise framed buildings and cantilevers. For example, besides the straightly anchored longitudinal bars, bent longitudinal bars are used in RC beams with large haunches (Fig. 1 [1]). Such beams are widely used for economic and aesthetic reasons. However, the number of experimental data to predict the shear behavior of RCHBs is insufficient. Moreover, rational and economical design method in the current JSCE specifications for concrete [2] has not been established yet. Since the effective depth of RCHB varies along the member axis from the support to the middle portion, it is very difficult to predict the shear capacity with the current shear design equations which is used for normal prismatic beams. Therefore, it is necessary to explore the shear resistance mechanism of RCHBs to ensure the shear behavior.

In the previous research reported by Tena-Colunga et al. [1], it was concluded that the shear capacity of RCHBs without shear reinforcement was affected mainly by the inclination of haunched portion and the effective depth at the mid span. However, the effect of the position of haunched portion which can have an important role in shear resistance mechanism of RCHBs and the effect of the concrete cover have not been investigated. Hence, in this study, the effects of the position of haunched portion from the loading point and the concrete cover on the shear behavior of RCHBs without shear reinforcement were investigated.

2. EXPERIMENTAL PROGRAMS

2.1 Test Specimens

Figure 2 and Table 1 illustrate the details of tested beams, including the dimension and reinforcing bars arrangement of RCHBs. The shear span (a) was 650 mm and effective depth was varied from 250 mm (d_s) to 200 mm (d_m) along the member axis. Consequently the shear span to effective depth ratio also varied from 2.6 to 3.25. All the specimens were designed to fail in the left shear span by providing stirrups only in the right shear span as shown in Fig. 2. The experimental parameters of these four beams were the positions of the haunched portions from the loading point, which were also used to name the specimens. For example, in the beam H-100, H means a haunched beam and 100 represents the distance between the haunched portion and loading point (b). In the beam HN-200, the haunched tensile longitudinal bars similar to the beam H-200 were provided. However, the concrete portion was not haunched, so that the uniform cross section throughout the beam could be obtained.



Fig. 1 RC building with haunched beams constructed in Mexico City

*1 Graduate Student, Dept. of Civil Engineering, Tokyo Institute of Technology, JCI Member

*2 Assistant Prof., Dept. of Civil Engineering, Tokyo Institute of Technology, Dr. E., JCI Member

*3 Prof., Dept. of Civil Engineering, Tokyo Institute of Technology, Dr. E., JCI Member

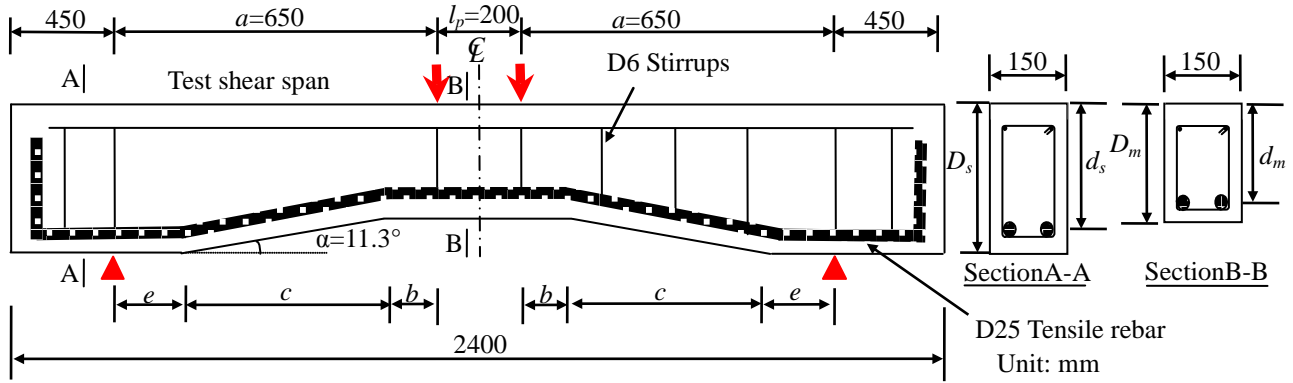


Fig. 2 Typical specimen detail

Table 1 Specimens details and material properties

Specimen	f_c' (N/mm ²)	a (mm)	b (mm)	c (mm)	e (mm)	l_p (mm)	D_s (mm)	d_s (mm)	D_m (mm)	d_m (mm)	a/d_s	a/d_m
H-100	33.6	650	100	250	300	200	300	250	250	200	2.6	3.25
H-200	29.6		200									
H-300	36.7		300									
HN-200	28.6		200									

f_c' : compressive strength of concrete; a : shear span; b : distance between loading point and beginning of haunched portion; c : length of haunched portion; e : distance between support and end of haunched portion; l_p : distance between two load points; D_s : beam depth at support; d_s : effective depth at support; D_m : beam depth at mid span; d_m : effective depth at mid span.

Table 2 Mix proportion of concrete

G_{max} (mm)	W/C	Unit weight (kg/m ³)				
		W	C	S	G	AE
20	0.60	178	297	847	946	0.446

G_{max} : maximum size of coarse aggregate; W: water; C: cement; S: fine aggregate; G: coarse aggregate
AE: air-entraining water-reducing agent.

2.2 Materials

In all four specimens, the longitudinal D25 tensile bars having yield strength of 411 N/mm² were used. The inclination of tensile steel bars, α was fixed to 11.3 degrees based on the dimension of a real structure with large haunches as well as considering the feasibility of the framework. The D6 stirrups of yield strength 277 N/mm² were arranged at the spacing of 200 mm in the non-test shear span to ensure the failure of the test shear span. Two round bars having a diameter of 6 mm and yield strength of 328 N/mm² were used as compression bars.

To obtain the concrete strength of 30 N/mm², high-early strength Portland cement, fine aggregates, coarse aggregates, and air-entraining water-reducing agent were mixed in proportion as shown in Table 2.

2.3 Loading Test and Instrumentation

Specimens were subjected to a four-point bending test with simply-supported condition as illustrated in Fig. 2. Steel plates with 50 mm width were placed on the pin-hinge supports. Teflon sheets and grease were inserted between the specimen and supports in order to prevent the horizontal friction. At loading points, the steel plate with 65 mm width and

150 mm length were also placed. Figure 2 shows the detailed loading setup along with the locations of loading points.

During the four-point bending tests, the mid-span deflection was measured using four displacement transducers at the mid span and supporting points. The strain in tensile steel bars at various locations and strain of concrete in several sections were measured by attaching strain gauges on the surface of the tensile bars and concrete (Fig. 6(a)). Also the crack propagation on the surface of test-span during the loading test was captured by taking pictures.

3. EXPERIMENTAL RESULTS AND DISCUSSIONS

3.1 Crack Patterns

Figure 3 shows the crack patterns in the specimens at the peak load. The white dash lines represent the positions of the haunched tensile longitudinal bars in the RCHBs. For the first three beams H-100, H-200 and H-300, the cracks started from the haunched portion where the tensile rebars were bent and it proceeded along inclined rebars and towards the loading point. The absence of stirrups caused the lack of confinement in the test span of the

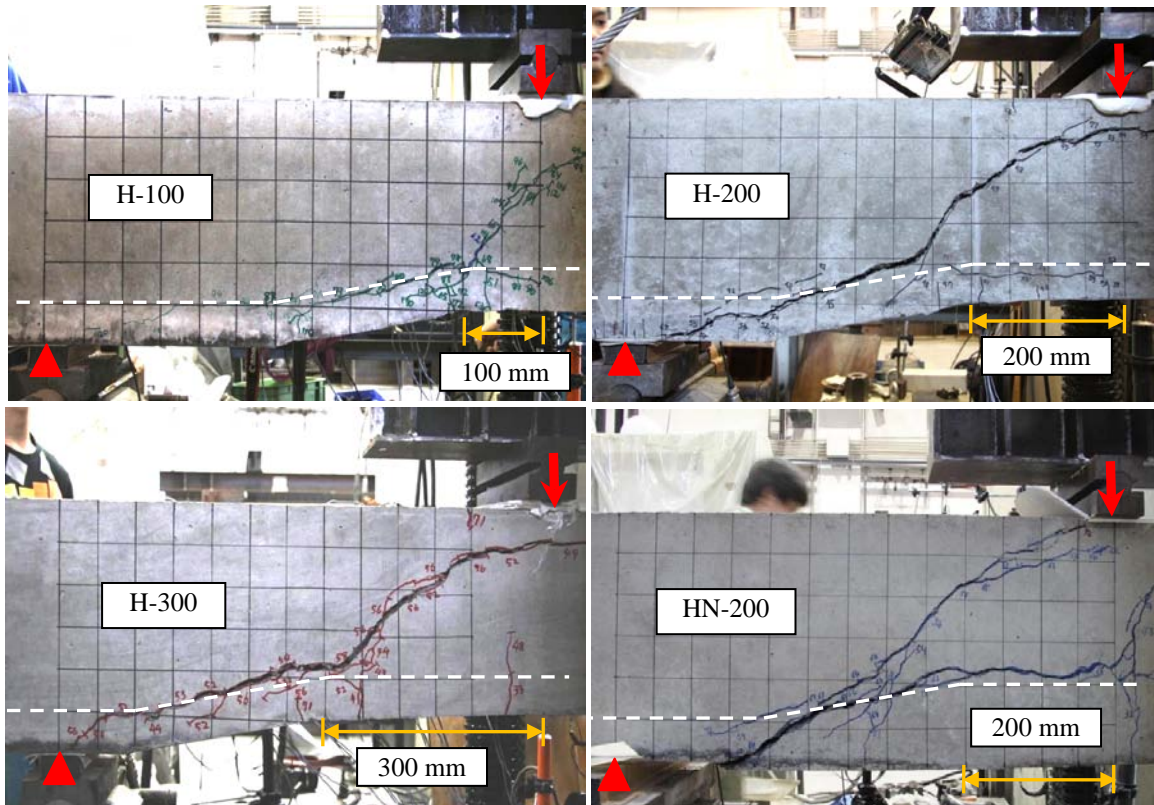


Fig. 3 Crack patterns in beams at peak load

specimens, due to which the inclined tensile bars tended to straighten on further loading and eventually led to debonding cracks along the inclined tensile bars in the haunched portion.

For the beam HN-200, the inclined shear crack started from the middle part of the haunched portion and propagated towards loading point. After the formation of the whole diagonal cracks, the debonding cracks along the tensile steel bars were suddenly occurred. However, all of the specimens failed in shear due to the crushing of concrete near the loading point.

3.2 Load-displacement Curves

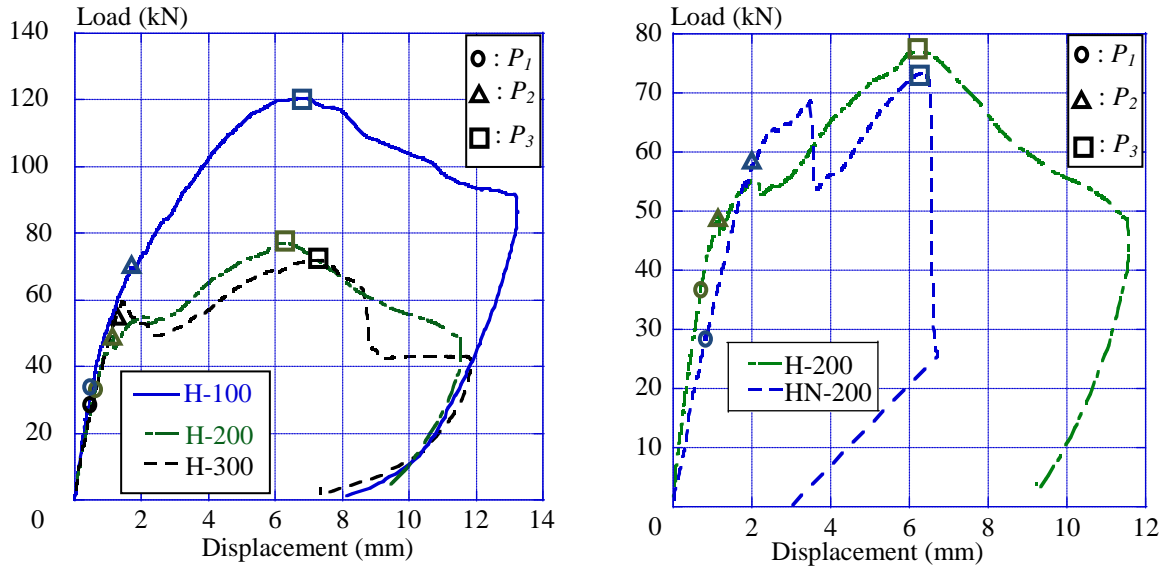
Figure 4 shows load-displacement curves and the summary of experimental results is shown in Table 3. The shear capacity of the beam H-100 was the largest (60.3 kN) among all the beams. The shear capacities of H-200, H-300 and HN-200 were smaller by 36%, 40% and 39% respectively than that of H-100. Although the cracks pattern and crack propagation of beam HN-200 were different from other RCHBs, the shear capacities of beam H-200, H-300 and HN-200 did not show significant difference. The reason behind such performances of the beams is discussed in the following sections.

3.3 Effect of the Haunched Shape and Inclined Tensile Rebars

On applying vertical load, tensile forces were generated in tensile rebars. As shown in Fig. 5, the vertical component (V_{hd}) of tensile force in the inclined

rebars at haunched portion acted in the opposite direction to the shear resistance offered by the concrete (V_c) at the section, resulting in negative contribution to the shear capacities of the beams. Hence, the applied shear force (V) became smaller than the actual shear resisted by concrete (V_c), causing the early occurrence of diagonal cracks in the beams. Being H-200 and H-300 slender beams ($a/d > 2.5$), the diagonal cracks occurred relatively early and suddenly than that of H-100. The load dropped after the formation of the whole diagonal cracks, just as indicated by the drop of the load in Fig. 4. However, due to the presence of haunches as well as the debonding cracks, the arch action was developed in the test span, resulting in gradual increase of load after diagonal cracks until the peak, which can be observed in the load-displacement curves of all the specimens.

Figure 6 shows an example of arch action in the beam HN-200. With the strain gauges attaching on the surface of a concrete beam for three sections in the shear span, the distribution of the strain for these three sections just before the peak load can be derived, as shown in Fig. 6(a). The positive value of the strain means tension, while the negative value of the strain means compression in concrete. The dash dot line represents the interface between compression and tension or the boundary of the compression zone. The slopes of the strain distributions indicate the concentration of compression force near the loading point. Consequently it also indicates that the area of compression zone was relatively smaller near the



P_1 : Load at flexural crack; P_2 : Load at diagonal crack; P_3 : Peak load

Fig. 4 Load-displacement curves

Table 3 Summary of experimental results

Specimen	P_1 (kN)	P_2 (kN)	P_3 (kN)	V (kN)
H-100	36	69	120.5	60.3
H-200	37	48	77.1	38.5
H-300	33	56	71.9	36.0
HN-200	28	58	73.3	36.7

P_1 : Load at flexural crack; P_2 : Load at diagonal crack
 P_3 : Peak load; V : Shear capacity

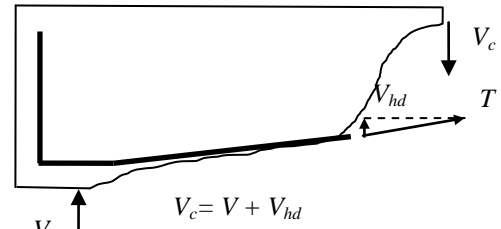


Fig. 5 Free body of haunched beam

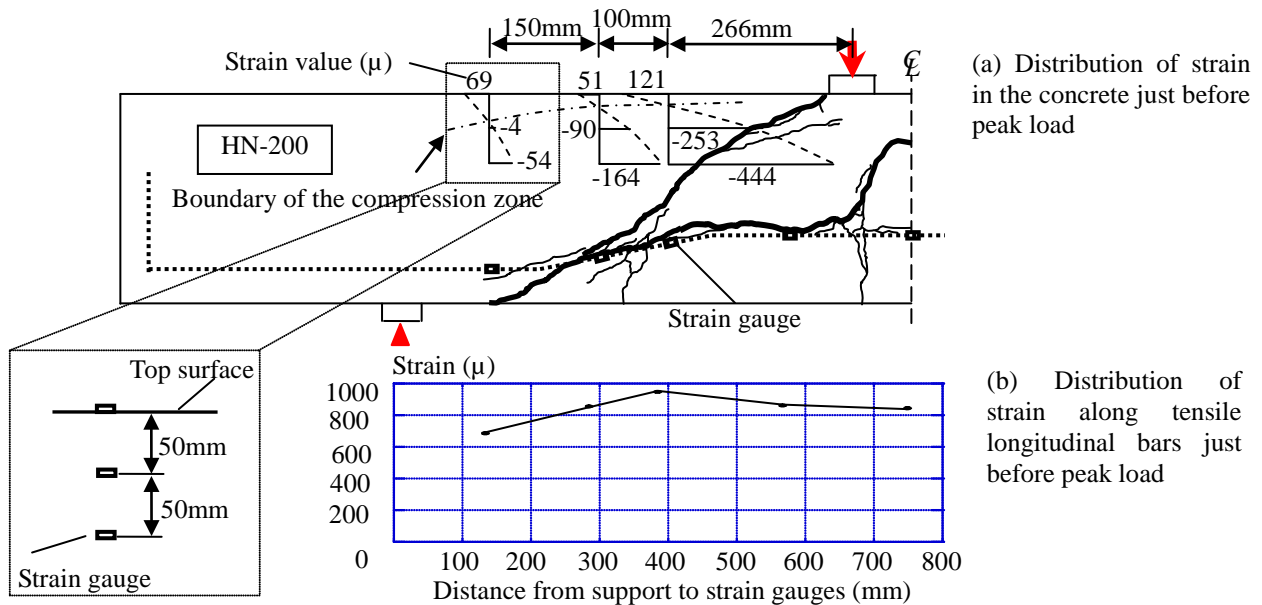


Fig. 6 Arch action in the beam HN-200

loading point than that near the support. The resultant force direction in the compression zone was assumed to be from the loading point to the support which matched with the distribution of the strain in the concrete. On the other hand, the distribution of the strain along the tensile longitudinal bars just before the peak load is shown in Fig. 6(b). Except the strain near the support, the values of other strain gauges in the shear span were

same or even larger than the value of the strain at the mid span. This phenomenon also indicates the tensile force in the tensile rebars was almost same, which is one of the evidences for arch action [3, 5].

3.4 Effect of the concrete cover

Although the haunched tensile longitudinal bars of the beam H-200 and HN-200 were identical, the

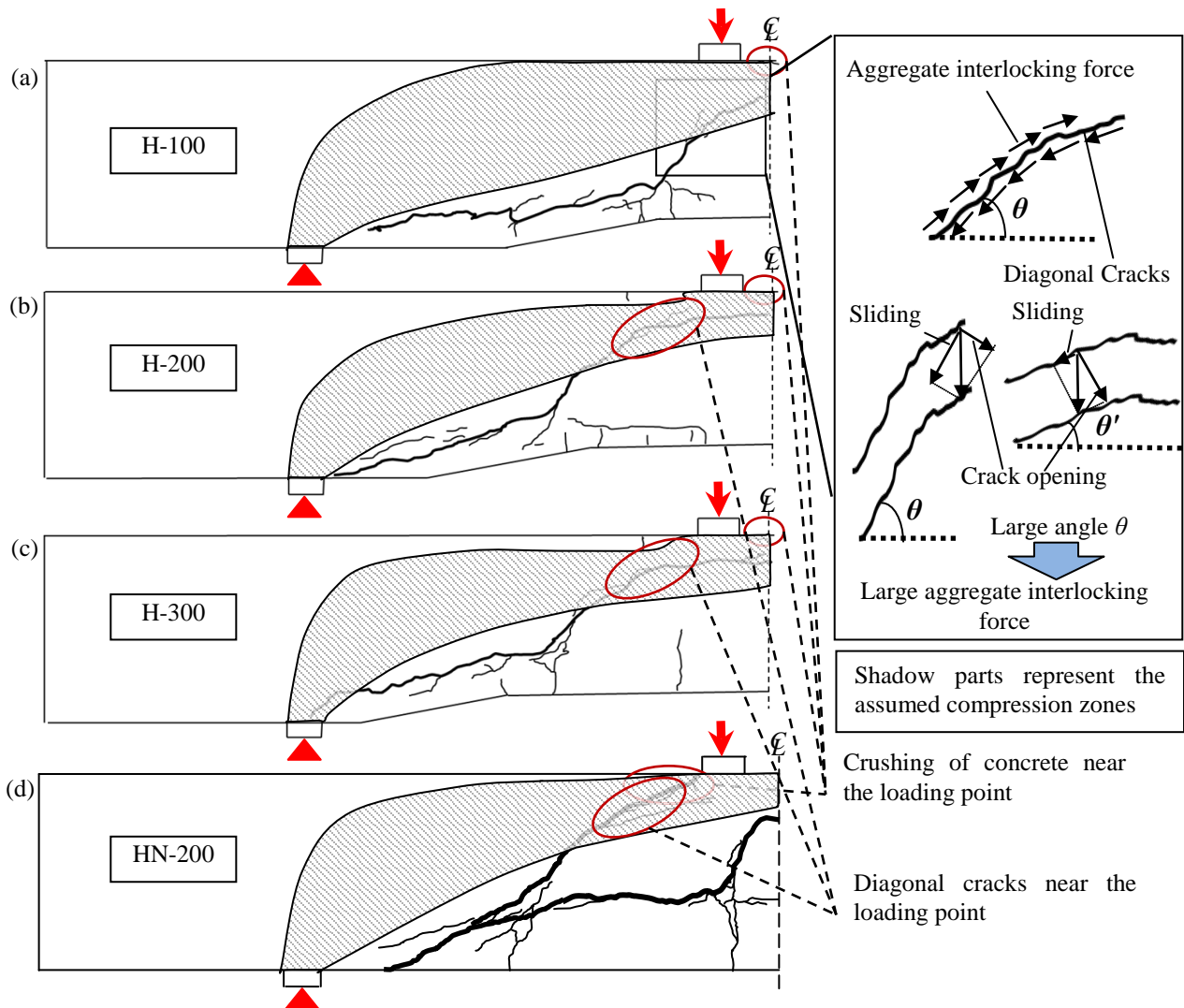


Fig. 7 Contribution of arch action and aggregate interlock

cover concrete in HN-200 was thicker than that in H-200. Hence, the effect of the concrete cover could be analyzed by comparing the performances of the beams H-200 and HN-200.

For the beam HN-200, the thick concrete cover at the mid span provided limited constrain at the beginning of the loading test and mitigated the negative effect of the inclined tensile steel bars till the tensile force in the steel bars was not very large. The diagonal crack gradually propagated and the load at diagonal cracks became 21% larger than that of beam H-200. However, due to the absence of shear reinforcement, the confinement provided by the concrete was still not enough at the higher load. When the load was increased and the debonding cracks suddenly occurred, the load dropped from 68 kN to 53.7 kN, which means the bond was lost and the redistribution of internal force occurred. It led to the similar situation as in the beam H-200 that arch action came into action and resisted the additional load.

3.5 Arch action, shear capacity and failure modes

The difference in crack propagation behavior was responsible for the different load-displacement curves, higher load at diagonal crack and higher shear

capacity of the beam H-100. Since the haunched portion of the beam H-100 was near the loading point compared with the other beams (Fig. 7(a)), the generation of diagonal cracks was shifted near the loading point. This shifting of the diagonal cracks made both the angle of the diagonal crack to the member axis (θ) and the concrete portions above the diagonal crack, particularly the area near the loading point, larger (Fig. 7(a)). Since the diagonal crack areas were in the middle height of the beams, near the neutral axis, the bending moment had little effect on the crack opening. Thus, when the angle of diagonal crack was large, for the same displacement, the shear force contributed more sliding along the cracks geometrically than the crack opening (Fig. 7). In such case, small crack opening and large sliding eventually caused the large aggregate interlocking force. Because of the large aggregate interlocking force, the load at the diagonal crack of H-100 was larger than those of other beams which could be found from the load-displacement curves in Fig. 4. In addition, no drop of load was observed in the beam H-100 when the whole diagonal crack was formed. It eventually slowed down the propagation of diagonal cracks with small crack width in the beam H-100.

By measuring the strain distributions at several sections of the concrete beams and along the tensile steel bars, it was found that, similar to the beam HN-200, in the other three specimens, an arch action was also developed in the shear span. The upper boundaries of the compression zones in these three beams were fixed with the same method shown in Fig. 6(a). As the lower boundary was not measured, Fig. 7 is just a schematic figure, and the shadow parts in it represent the assumed compression zones in all four beams before the peak load. In the beams H-200, H-300 and HN-200, since the values of the strain gauges below the diagonal cracks near the loading point were also in compression, the assumed compression zones of these beams passed the cracks.

As the area of the compression zone is small near the loading point and relatively large near the support, the compression area near the loading point is more important for the arch action. The large concrete portions above the diagonal crack in the beam H-100 resulted in the large compression zone, especially the area near the loading point. It made the arch action resist the shear force significantly and eventually led to the higher shear capacity. For the other three beams, as shown in Fig. 7(b), (c) and (d), the area of compression zone near the loading point was relatively smaller than that of H-100. Based on the compression-softening theory, the cracks in the compression zone in these beams also reduced the compression strength of the concrete [4]. Therefore, the developed arch action in these beams did not contribute significantly in resisting shear force. So, relatively smaller increase in shear capacity after the occurrence of diagonal cracks was observed in H-200, H-300 and HN-200.

In addition, for the beam HN-200, before the crushing of concrete near the loading point, the diagonal cracks were different but still similar to that of H-200. Consequently, the compression zone and the effect of developed arch action in the beam HN-200 were also similar to those of the beam H-200. As the shear capacities of these two beams were almost same with each other, it indicates that the situations of these two beams became almost same after the occurrence of debonding cracks and the concrete cover did not make any contributions for shear capacity.

For normal prismatic slender beams ($a/d > 2.5$) without shear reinforcement, the failure mode is diagonal tension failure. The load cannot increase after the diagonal cracks occur and the peak load is almost same as the load of diagonal cracks [1, 5]. However, based on the previous observations, the failure modes of all the four RCHBs were considered as more like the shear compression failure that an inclined compression zone formed in the shear span and the arch action worked to resist the shear force. Because of this, the load increased after the diagonal cracks until the crushing of concrete near the loading point. Although the shear capacities of four beams were different, the existence of compression zone, arch action and increase

of shear capacity after diagonal cracks indicate the shear compression failure.

Although the positions of haunched portion in the beam H-200 and the beam H-300 were different, the differences of shear capacities were not as large as that of H-100. It indicates that the effect of haunched portion may have some affecting range, which will be investigated in the future research work.

4. CONCLUSIONS

- (1) For the RC haunched beams (no stirrups) with normal concrete cover, the cracks started from the haunched portion where the tensile rebars were bent and it proceeded along inclined rebars and towards the loading point.
- (2) The thick concrete cover of RC haunched beams (no stirrups) provided limited constraint at the beginning and mitigated the negative effect of the inclined tensile rebars. However, after the occurrence of the debonding cracks, it came back to the similar situation with the RC haunched beams (no stirrups) with normal concrete cover where arch action came to resist the shear force.
- (3) Apart from the inclination of the haunched tensile longitudinal steel bars and the effective depth of RCHBs, the positions of haunched portions affect the shear capacities significantly.
- (4) The inclined tensile rebars make negative contribution on the shear capacity, while the haunched shape of RCHBs and debonding cracks result in arch action even in slender beams, eventually causing the shear compression failure. However, the contributions of arch action are different in different beams due to the variation in crack patterns.

REFERENCES

- [1] Tena-Colunga, A., Archundia-Aranda, H.I. and Gonzalez-Cuevas, O.M., "Behavior of Reinforced Concrete Haunched Beams Subjected to Static Shear Loading", *Engineering Structures*, Feb. 2008, Vol. 30, No. 2, pp. 478-492.
- [2] JSCE, "Standard Specifications for Concrete Structures-2007, Structural Performance Verification", JSCE Guidelines for Concrete, No. 15, Dec. 2010.
- [3] Michael D. Kotsovos, "Compressive Force Path Concept: Basic for Reinforced Concrete Ultimate Limit State Design", *ACI Structural Journal*, Jan.-Feb. 1988, Vol. 85, No. 1, pp. 68-75.
- [4] F. J. Vecchio, M. P. Collins, "Compression Response of Cracked Reinforced Concrete", *ASCE Journal of Structural Engineering*, Dec. 1993, Vol. 119, No. 12, pp. 3590-3610.
- [5] James K. Wight, James G. MacGregor, "Reinforced Concrete: Mechanics and Design", Prentice Hall, Sep. 2011, 6 edition, pp. 214-215.